

Extended Dust Emission from Nearby Evolved stars

Thavisha E. Dharmawardena^{1,2}, Francisca Kemper¹, Peter Scicluna¹,
Jan G. A. Wouterloot³, Alfonso Trejo¹, Sundar Srinivasan¹,
Jan Cami^{4,5}, Albert Zijlstra^{6,7}, Jonathan P. Marshall¹ and the
NESS collaboration

¹Academia Sinica Institute of Astronomy and Astrophysics, 11F of AS/NTU
Astronomy-Mathematics Building, No.1, Sect. 4, Roosevelt Rd, Taipei 10617, Taiwan, R.O.C.

² Graduate Institute of Astronomy, National Central University, 300 Zhongda Road, Zhongli
32001, Taoyuan, Taiwan, R.O.C.
email: tdharmawardena@asiaa.sinica.edu.tw

³East Asian Observatory, 660 N A'ohoku Place, Hilo, Hawaii 96720, USA

⁴Department of Physics and Astronomy and Centre for Planetary Science and Exploration,
The University of Western Ontario, London, ON N6A 3K7, Canada

⁵SETI Institute, 189 Bernardo Ave, Suite 100, Mountain View, CA 94043, USA

⁶Jodrell Bank Centre for Astrophysics, School of Physics and Astronomy, University of
Manchester, Oxford Road, Manchester M13 9PL, UK

⁷Laboratory for Space Research, University of Hong Kong, Pokfulam Road, Hong Kong

Abstract. We derive azimuthally-averaged surface-brightness profiles of 16 AGB stars in the far-IR and sub-mm with the aim of studying the resolved historic mass loss in the extended circumstellar envelope. The PSF-subtracted extended component fluxes were found to be $\sim 40\%$ of the total source flux. By fitting SEDs at each radial point we derive the dust temperature, column density and spectral index of emissivity via Bayesian inference. The measured dust-to-gas ratios were somewhat consistent with canonical values however with a large scatter.

Keywords. stars: AGB and post-AGB - stars: circumstellar matter - stars: mass-loss

1. Introduction

At present many studies involving evolved-star dust production take into account only the present day mass-loss rates via mid-IR observations. This treatment ignores an older cooler dust component emitted during historic mass loss events. Further, in many cases evolved stars are treated as quasi-stable systems not taking into account the variations of historic mass loss. This cooler dust component and its variations are only observable at longer wavelengths such as in the far-IR and sub-mm. Therefore at present we do not have a clear understanding of the extended circumstellar envelopes of evolved stars formed as a result of the historic mass loss. Evidence for the presence of this historic dust mass component is reported by Cox *et al.* (2012) who presented a large sample of evolved stars in the far-IR using Herschel/PACS observations at 70 μm and 160 μm . These observations show dust envelopes with extensions out to $\sim 1' - 2'$.

We analyse sixteen evolved stars (5 C-rich, 9 O-rich, and 1 S-type Asymptotic Giant Branch (AGB) stars, and 1 red supergiant (RSG)) with the goal of understanding the historic mass loss component (Dharmawardena *et al.* 2018, and Dharmawardena *et al.*, in prep). The analysis was carried out using new sub-mm observations with the JCMT/SCUBA-2 instrument combined with existing far-IR Herschel/PACS observations

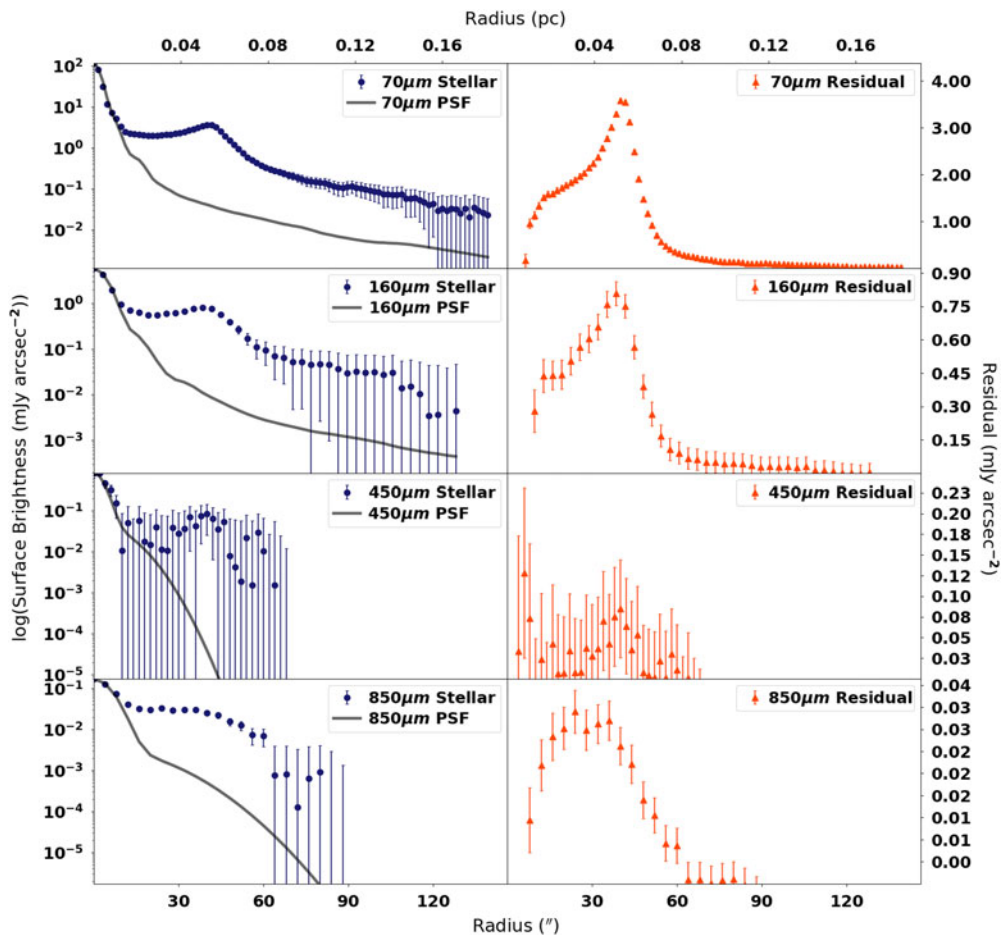


Figure 1. Surface brightness and residual profiles of U Ant. Right hand panels: The blue dashed lines represent the source surface brightness profiles and the grey solid lines represent the PSF profile of the instrument at the given wavelength; Left hand panels: PSF subtracted residual profiles for each wavelength (Dharmawardena *et al.*, in prep.).

from the MESS survey. This analysis was a pilot study for the Nearby Evolved Stars Survey (NESS, <https://evolvedstars.space>) which aims to statistically analyse the extended dust and gas emissions in a volume limited sample of nearby evolved stars.

2. Azimuthally-averaged surface-brightness profiles

By generating azimuthally-averaged surface-brightness profiles we were able to measure the extent of the circumstellar envelope and its surface-brightness properties. The sources on average have radii at 3σ surface brightness limits of $\sim 40'' - 50''$ with a maximum of $80''$ at the SCUBA-2 wavelengths. A significant component of the total flux, an average of $\sim 40\% - 50\%$, was concentrated within the PSF-subtracted extended source component. This shows the significance of the cool historic dust component when analyzing the mass-loss rates and dust production rates of these evolved stars even in a statistical sense. Additionally, the surface brightness profiles, as well as the PSF-subtracted residual profiles, show circumstellar envelope structure for several sources. For example, as shown in Fig. 1 we see clear evidence for the detached dust shell of U Ant in the form of enhancements in the surface-brightness and residual profiles at all four wavelengths.

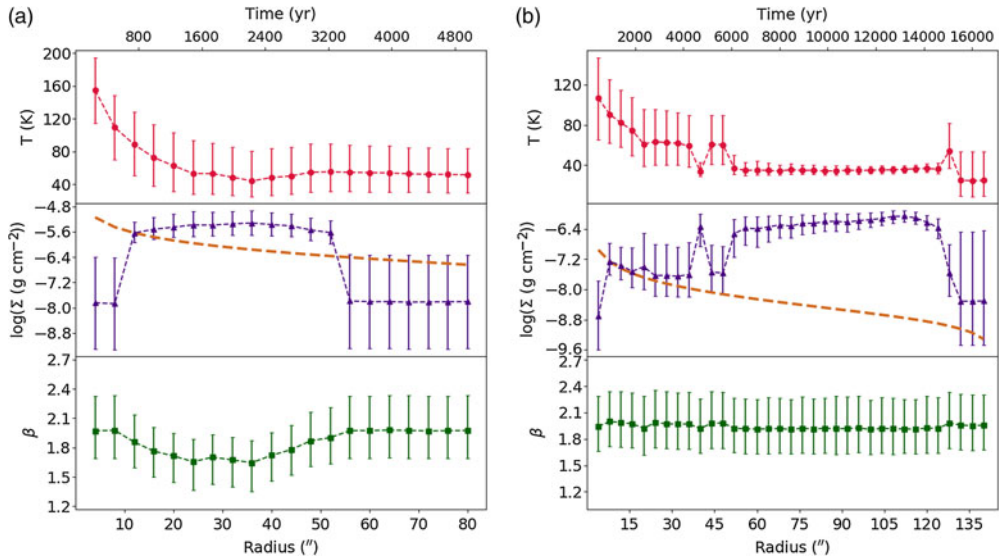


Figure 2. SED fitting results of U Ant (left) and U Hya (right); Top: Temperature (T) radial profiles; Middle: Dust mass column density (Σ) radial profile. The orange dashed line represents the expected dust mass column density for a uniform mass-loss rate; Bottom: The spectral index of dust emissivity (β) profile (Dharmawardena *et al.* 2018, and Dharmawardena *et al.*, in prep)

3. Radial Variation in the Dust Properties

We derive dust mass properties as a function of radius for each source by fitting a single-temperature modified blackbody at each radial point to the four point SED created by combining the residual profiles at all four wavelengths. The SED fitting was carried out using the python MCMC package *emcee*. The derived radially dependent dust temperature (T), spectral index of the dust emissivity (β), and the dust column density (Σ) profiles are used to probe the dust mass-loss history and detect changes in physical properties of dust as a function of radius, thus time.

The derived parameter profiles for U Ant and U Hya are presented in Fig. 2. All three parameter profiles had common features which were present throughout most of the sample. The T profiles initially show a decreasing gradient consistent with a centrally heated optically thin dust mass. This is followed by a near flat gradient consistent with a dust mass heated by the interstellar radiation field (ISRF).

The Σ profiles deviate from the corresponding profile expected for constant mass-loss rate (MLR), hence showing that these sources underwent mass-loss modulations during their lifetimes. The features seen in the profiles, for example the enhancements seen in the middle panels of Fig. 2 of the detached shell sources U Hya and U Ant, correspond to these mass loss modulations. Using these profiles we can therefore derive the look-back time at which the mass loss modulations occur. We find that the thermal pulse which gave rise to the detached shells of U Hya and U Ant occurred $\sim 14000 \pm 1000$ and $\sim 3200 \pm 500$ years ago in look-back time. We observe large scale mass-loss variations up to time scales of $\sim 7400 \pm 1000$ yrs, comparable to thermal pulse time scales reported by Olofsson *et al.* (1990), but much larger than modulations reported by Marengo *et al.* (2001).

Due to the smaller extent of the detections in the SCUBA-2 observations when compared to the PACS observations, the majority of our β profiles were prior dominated following a flat profile similar to what is observed in the case of U Hya (see bottom

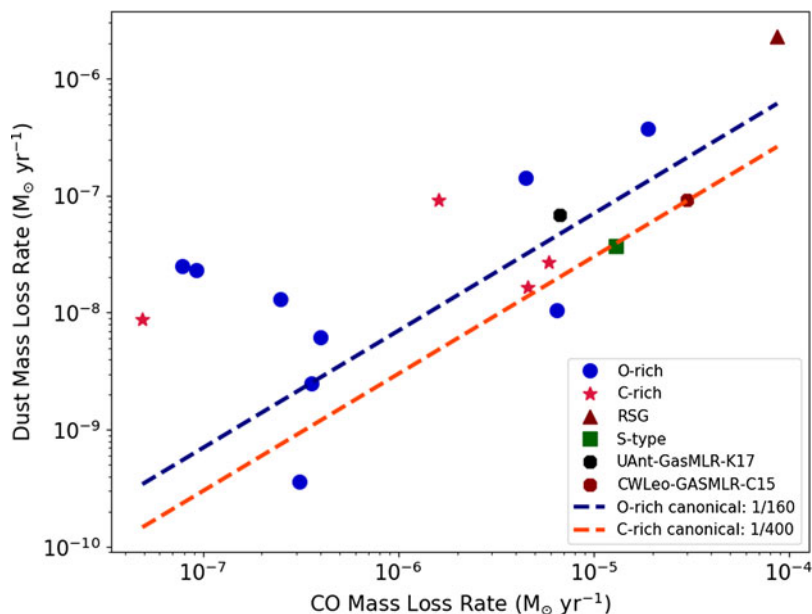


Figure 3. Gas MLR versus dust MLR. Blue circles: O-rich AGB stars; crimson stars: C-rich AGB stars; green square: S-type AGB star; maroon triangle: RSG; orange dashed line: the accepted dust-to-gas ratio of 1/400 for C-rich sources; and blue dashed line: the accepted dust-to-gas ratio of 1/160 for O-rich sources. (Dharmawardena *et al.* 2018)

panel of Fig. 2b). However for several sources with SCUBA-2 detection extents comparable to those of the PACS extents we see the variation of dust properties with time reflected in the variations in β profile. We find that the β limits in the detectable region of IRC+10216 is consistent with the presence of graphitic dust, and in the case of U Ant the dust is composed of amorphous carbon grains (see bottom panel of Fig. 2a).

4. Dust masses and dust-to-gas ratios

We derive the dust masses of the extended component by integrating the Σ profile. We find that these masses are on average ~ 5 times greater than those predicted by GRAMS radiative transfer models (Srinivasan *et al.*, 2012). We attribute this to the fact that GRAMS utilizes only the mid-IR observations which are sensitive only to the warmer central present day mass-loss, not taking into account historic mass loss or its modulation. This shows the importance of taking into account the cooler historic dust-mass component when analyzing mass output by evolved stars into the ISM.

By extrapolating the central point gas mass loss rates reported in De Beck *et al.* (2010) we derive the total gas masses up to the same look-back time period as that of the dust masses we derive. As shown in Fig. 3, the derived dust-to-gas ratios are somewhat consistent with the canonical dust-to-gas ratios presented in Knapp & Morris (1985). However we also see a large scatter in the derived ratios. Again, this is most likely due to the fact that while we take into account the historic mass loss modulations when determining dust masses, it is not possible to do so for the gas masses as we only had central present day gas mass-loss rates. For the case of U Ant and IRC+10216 where we did have a gas mass-loss rate determined via resolved observations which took into account its extended gas emission we find the dust-to-gas ratios changing significantly from the previous measurement and being more consistent with the canonical.

5. Summary

By analysing the resolved extended dust emission of sixteen evolved stars in the far-IR and sub-mm we find an extended cooler dust component resulting from historic mass loss. We find a significant portion of the total source flux is found within this extended component. The variations in total dust masses and dust-to-gas ratios from those derived from present day mass loss rates and mid-IR observations, show the importance of taking this historic cooler dust mass component and the resulting mass loss modulation effects (variations in the circumstellar envelope structure) into account when determining mass output to the ISM by evolved stars.

References

- Cox N. L. J., *et al.*, 2012, *A&A*, 537, A35
 De Beck E., Decin L., de Koter A., Justtanont K., Verhoelst T., Kemper F., Menten K. M., 2010, *A&A*, 523, A18
 Dharmawardena T. E., *et al.*, 2018, *Monthly Notices of the Royal Astronomical Society*, 479, 536
 Knapp G. R., Morris M., 1985, *ApJ*, 292, 640
 Marengo M., Ivezić Ž., Knapp G. R., 2001, *MNRAS*, 324, 1117
 Olofsson H., Carlstrom U., Eriksson K., Gustafsson B., Willson L. A., 1990, *A&A*, 230, L13

Discussion

SLOAN: You compared the dust mass in the mid-IR to the far-IR and got 5 times more dust in the far-IR. Perhaps it would be better to think in terms of rates. If the far-IR region samples 5 times the time, then the rates are the same. How much more time does the far-IR sample?

DHARMAWARDENA: We calculate the mid-IR dust masses by extrapolating to the same look-back time as those of the far-IR and sub-mm. Therefore the dust masses both are measured upto the same time and therefore analogous to measuring the differences in the rates.

MAERCKER: The density profile for U Ant goes in a lot further than would be expected from a detached-CSE.

DHARMAWARDENA: We find the SCUBA-2 850 μm observations peaks in the inner region as a result of the substructure of the outer shells projected to the inner region. The PACS on the other hand peaks at the location of the outer shells. As a result when we combine and compute SEDs as a function of radius we see a density enhancement which is wider than the thin outer shells.

SAHAI: What were the ‘canonical’ dust-to-gas ratios used for O-rich and C-rich stars, and did you use the standard dust opacities (if so, which ones)?

DHARMAWARDENA: 1. We use canonical values of 0.003 and 0.007 for C-rich and O-rich stars reported in Knapp and Morris 1985. 2. We use $\kappa_{\text{eff},160}^s = 26 \text{ cm}^2 \text{ g}^{-1}$ for C-rich and $8.8 \text{ cm}^2 \text{ g}^{-1}$ for O-rich (including RSG and S-type) by computing cross sections for spherical grains of $\sim 0.1 \mu\text{m}$ using ACAR optical constants for amorphous C-grains.